

A STUDY ON DEVELOPMENT OF STRESSES IN ANCHORAGE ZONE USING PARALLEL PROCESSING

P.K. Gupta* and R.N. Khapre

Civil Engineering Department, Indian Institute of Technology Roorkee, India

Civil Engineering Department, RKNEC Nagur, India

Abstract

This paper presents an investigation into the development of stresses in anchorage zone in prestressed post-tensioned concrete beam using the finite element analysis. A finite element computer code on the platform of a supercomputer PARAM 10000 is developed and employed for the present study. A parallel algorithm for matrix inversion method is developed and implemented in the presented finite element code. Concentric and eccentric prestressing forces are applied for prestressing of the beams. Effect of Poisson's ratio over the bursting tensile force developed in the anchorage zone is studied and an equation to compute the magnitude of bursting tensile force by incorporating the effect of Poisson's ratio is proposed. Development of spalling zone is also investigated and it was found that due to eccentric loading, stresses of higher magnitude were developed in this zone. Supercomputer PARAM 10000 is used to carry out present analysis and time reduction has been achieved by using multiple processors of the supercomputer PARAM 10000. At the end the performance of the developed parallel code is studied and presented.

Keywords: Anchorage zone; Spalling zone; Bursting tensile force; PARAM 10000

1. Introduction

In the prestressed post-tensioned concrete beam, anchorage zone is the zone in which complex stress development is observed. Along the axis of loading, transverse tensile stresses (σ_t) develops. The magnitude of this stress is sometimes higher than the permissible tensile stress in concrete at some location in the anchorage zone. Hence it may results bursting of concrete in the zone. Transverse tensile stresses are also developed in the regions around the free corners of the beam, which are generally designated as spalling zone. In the past few decades few researchers have attempted this problem using different techniques, which includes experimental methods [1,2], analytical techniques [3,4] and numerical methods [5-6] like Finite Element technique.

Zielinski and Rowe [1] presented results of surface strains measured on the concrete end

* E-mail address of the corresponding author: spramod_3@yahoo.com

block subjected to concentric prestressing forces. On the basis of their results, they gave an expression to calculate the magnitude of the bursting tensile force (F_{bst}) for different values of k (ratio of loaded area and cross-sectional area of the beam). This expression was then adopted and modified (factor of safety introduced) by the Indian Standard Code IS: 1343-1980². The effect of Poisson's ratio (ν) and eccentricity (e) of prestressing forces (P_k) over F_{bst} was not included in the given expression. Iyengar [3-4] analyzed the problem of anchorage zone using the equations of elasticity considering problem as 2-dimensional and 3-dimensional. They carried out the analysis for concentric as well as eccentric prestressing forces and compared the results with the available literature.

Yettram and Robbins [5] did investigation of anchorage zone stresses considering it as a 3-dimensional problem. They used finite element analysis (FEA) to determine the anchorage zone stresses. Their investigation does not prove the occurrence of spalling zone. Recently, Byung-Wan Jo [6] investigated the anchorage zone stresses by considering effects of various parameters namely cable inclination, position of anchor plate, and the modeling methods. They also carried out their analysis using finite element method (FEM) considering the problem as 2-dimensional as well as 3-dimensional and found that the 3-dimensional analysis gives slightly smaller values of stresses as compared to their 2-dimensional analysis. They suggested to adopt the results of 2-dimensional analysis to ensure the safety in the design.

Several research papers [7] are available which present the implementation of parallel computing technique in FEA. Literature shows that parallel solvers can successfully reduce the computational time in complex nonlinear dynamic finite element analysis as well as in simple linear elastic finite element analysis [8-10] of structural components. Kant and Shah [8] presented a parallel Cholesky solver to determine the solution of system of linear equation for analyzing the composite materials using FEM on supercomputer. Khan and Topping [9] presented a modified parallel Jacobi-conditioned conjugate gradient method for solution of linear elastic finite element system of equations. Thiagarajan and Aravamuthan [10] presented a preconditioned conjugate gradient finite element solver on 32-node Pentium II 350Mhz clusters.

An attempt has been made through this paper to present a computational Finite Element model to study the effect of Poisson's ratio and eccentricity of prestressing forces on development of stresses in anchorage zone and spalling zone in prestressed post-tensioned concrete beam. First the model has been verified by comparing the obtained results with the existing literature and there after it is used to carry out the simulation study by changing numerical values of k , e and ν to study their effect on stress distribution. On the basis of the obtained results an expression for computing bursting tensile force incorporating the Poisson's ratio is developed. As the present study involves numerous computations a supercomputer [11] is employed to save the computational time. A generalized computer program is developed using FEM on the platform of supercomputer PARAM 10000 with matrix inversion parallel solver to carry out linear structural analysis and used for the present analysis. The computational time reduction with increasing number of processors is obtained and discussed.

2. Idealization of the Problem

The problem of anchorage zone in prestressed post-tensioned concrete beam is idealized as 2-dimensional, plane stress problem. A rectangular beam of unit thickness is considered with the length of beam considered as twice of the depth of beam. Finite element method is used to analyze this problem. The discretized mesh consists of 4800 constant strain triangular elements with 2501 nodes each having two degree of freedom, hence resulting in global stiffness matrix of size 5002×5002 . In order to validate the results obtained by present investigation, comparison of obtained results is made with the results available in the literature. After ensuring that results of present investigation match well with literature, study was carried out considering different values of k and v to obtain their influence on the stress distribution in anchorage zone as well as spalling zone and on the bursting tensile force. For the present study, two cases are considered: Case I – Concentric prestressing force, where the value of k varied from 0.1 to 0.9 and the value of v varied from 0.0 to 0.3 (see Figure 1(a)). Case II – Eccentric prestressing force with the value of eccentricity varying from 0 to $0.8 d/2$ with constant value of $k = 0.1$ and $v = 0.15$ (see Figure 1(b)).

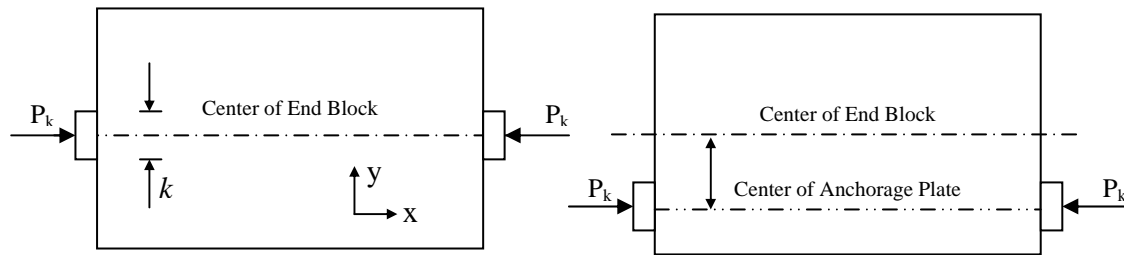


Figure 1. (a) Concentric (b) Eccentric loading on idealized prestressed concrete beam used in simulation study

3. Concentric Prestressing

Distribution of transverse tensile stress is used to compute the bursting tensile force. Area under the transverse tensile stress curve along the axis of loading gives the magnitude of bursting tensile force. Hence it is essential to compare the distribution of transverse tensile stress obtained with the present model with the literature. Figure 2(a) shows the comparison of transverse tensile stress distribution (σ_t) for a typical case of $k = 0.2$ and $v = 0.15$. Figure shows that the variation obtained by the present investigation almost matches with the variation obtained by Iyengar (2-dimensional). The variation obtained by Iyengar (3-dimensional) and Yettram and Robbins do not agree with the variation obtained by present investigation. It can be observed that the value of $\sigma_{t(max)}$ obtained by Yettram and Robbins and Iyengar (3-dimensional) are nearly 1.5 times and 2.5 time of the present analysis. It can be observed that the variation of transverse tensile stress obtained in present investigation is more realistic by incorporating the effect of v as compared to the findings of Iyengar (3-dimensional, 2-dimensional) and Yettram and Robbins.

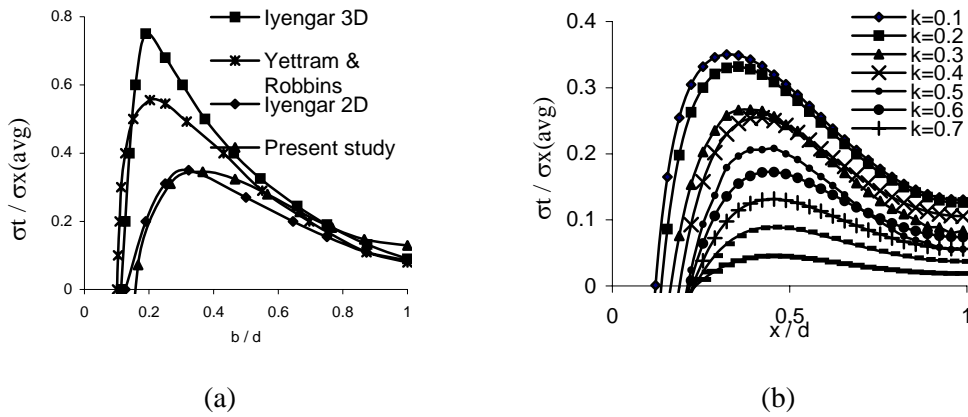


Figure 2. (a) Comparison and (b) Variation of transverse tensile stress distribution

In order to get the in-depth stress distribution, various simulation studies were carried out and several distribution curves were produced for concentric prestressing forces at different values of k ranging from 0.1 to 0.9 and ν ranging from 0 to 0.3. Figure 2(b) shows a typical variation in σ_t within the anchorage zone for a constant value of $\nu = 0.15$. One can observe that the magnitude of maximum transverse tensile stress ($\sigma_{t(\text{max})}$) in the anchorage zone starts decreasing with the increase in the value of k . One can also observe that as the value of k increases, the locations of zero and maximum transverse tensile stress points start moving away from the loaded face and close to the center of beam [12].

4. Eccentric Prestressing

To study the effect of eccentric prestressing forces, a particular set was considered which has $k = 0.1$ and $\nu = 0.15$. At the same time, the value of e was varied from 0.1 to 0.9. Figure 3 shows the variation in σ_t along the axis of loading for $k = 0.1$ and $\nu = 0.15$. It can be observed from this figure that as the eccentricity of prestressing force increases the magnitude of $\sigma_{t(\text{max})}$ inside the anchorage zone also increases but its location shifts towards the loading face [13].

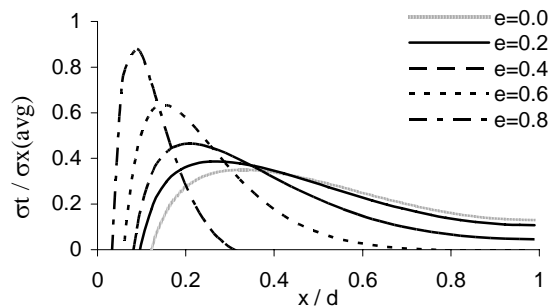


Figure 3. Variation in transverse tensile stress along the axis of loading

5. Bursting Tensile Force (F_{bst})

The Bursting tensile force F_{bst} can be found by calculating the total area under the transverse tensile stress curves (see Figure 2(b)). It is need less to say that for concentric prestressing forces the value F_{bst} decreases with the increase in value of k . Figure 4(a) shows the variation in F_{bst} with variation of ν . One can observe that as the value of ν increases, the magnitude of F_{bst} also increases. Significant variation in F_{bst} with ν can be observed at lower values of k .

Figure 4(b) shows the variation in F_{bst} with e for eccentric prestressing case. It shows that the magnitude of F_{bst} decreases with the increase in value of e . The magnitude of maximum F_{bst} can be observed at concentric loading conditions ($e = 0.0$). It can be seen from Figure 3 that the area under the transverse tensile stress curve reduces with increase in value of e , which ultimately results in reduction in bursting tensile force. Hence to insure the safety of the prestressed concrete beam, the effect of eccentricity can be ignored while computing the magnitude of bursting tensile force.

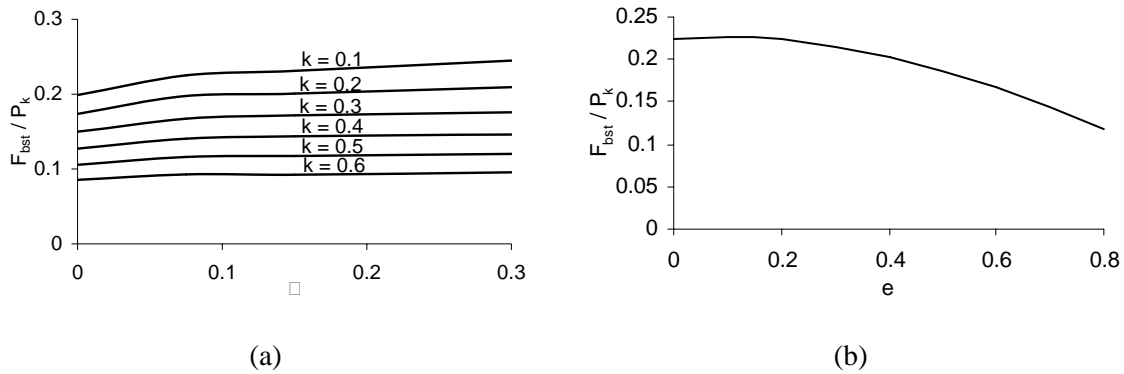


Figure 4. Variation in F_{bst} with (a) Poisson's ratio and (b) Eccentricity

Multiple regression analysis was carried out to obtain the correlation between F_{bst} and ν ignoring the effect of e . The following two expressions were obtained

$$F_{bst} = P_k (0.239 - 0.267 k + 0.075 \nu) \tag{1}$$

and

$$F_{bst} = P_k (0.229 - 0.238 k + 0.152 \nu - 0.22 k \nu) \tag{2}$$

The R^2 values obtained for equation 1 and 2 were 0.98 and 0.988 respectively. It can be noted that these equations also include the effect of Poisson's ratio in calculation of F_{bst} which is ignored in the equation (Eq. 3) given in Indian Standard Code IS:1343-1980.

$$\frac{F_{bst}}{P_k} = 0.32 - 0.3 \frac{y_{po}}{y_o} \quad (3)$$

where,

$$\frac{y_{po}}{y_o} = k$$

It can be seen that Eq. (2) is more accurate as compared to the Eq. (1). Hence Eq. 2 is followed to compare the results with the available literature. The comparison of variation in F_{bst} in the beam for different values of k for a constant value of $\nu = 0.15$ is shown in Figure 5. The magnitude of F_{bst} obtained by present investigation will always be lower than the magnitude of F_{bst} obtained using the equation given in the Indian Standard Code IS: 1343-1980 for all values of k . It is clear from this figure that the magnitude of F_{bst} obtained by Iyengar (2-dimensional) is slightly higher and Iyengar (3-dimensional) is slightly lower than the magnitude of F_{bst} obtained by present investigation. Among all three investigations, the magnitude of F_{bst} obtained by Yettram and Robbins is the lowest. It is very clear from this figure that the magnitude of F_{bst} is smaller when problem was idealized as 3-dimensional [3,5] while higher when problem was idealized as 2-dimensional [4] as compared to the present investigation. It is also known that the effect of ν was ignored in all these investigations in computation of magnitude of F_{bst} , which is considered in the present investigation. Therefore more accurate magnitude of F_{bst} could be obtained by using proposed expression.

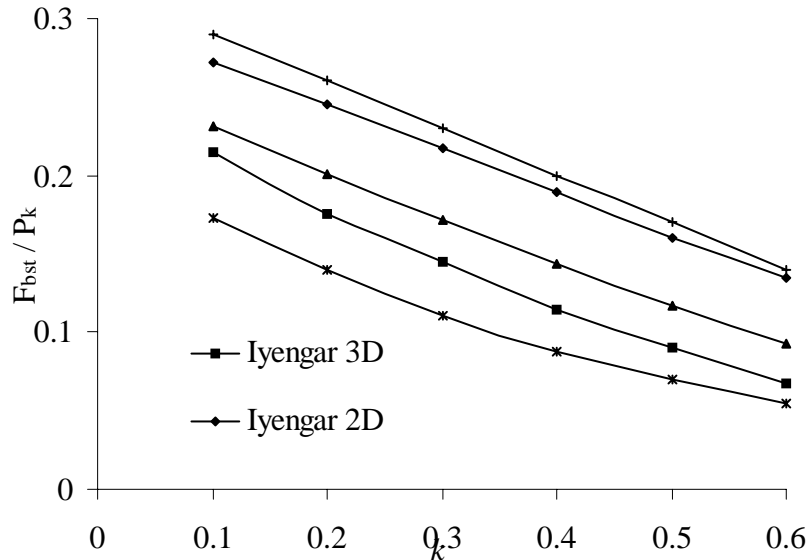


Figure 5. Comparison of variation in bursting tensile force

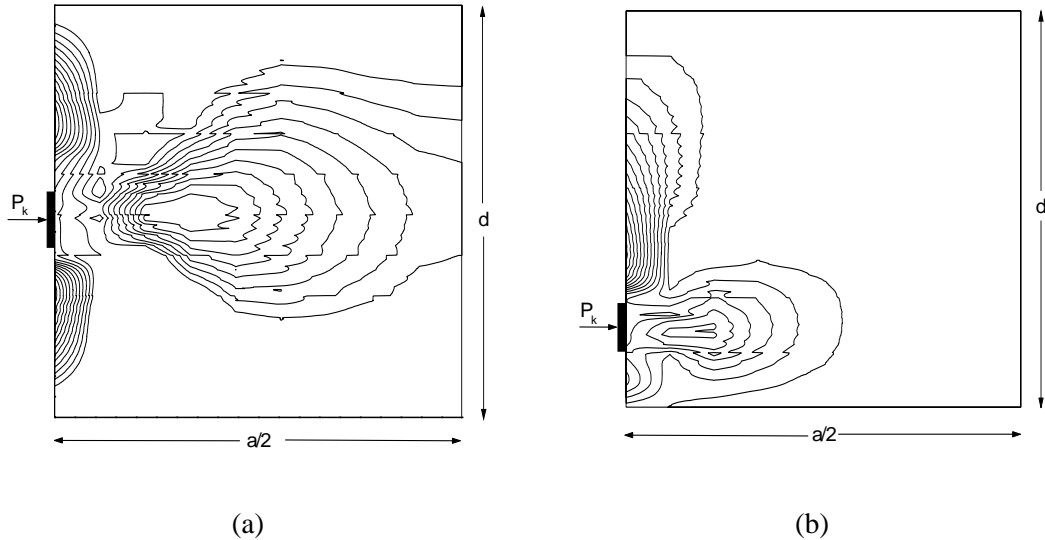


Figure 6. Stress contours for σ_t for $k = 0.1$, $\nu = 0.15$ (a) at $e = 0.0$ and (b) at $e = 0.8$

6. Spalling Zone

Figure 6(a) and Figure 6(b) shows the stress contours of σ_t for concentric and eccentric prestressing cases respectively. It can be observed from these figures that spalling zone does exist near the free corners of the beam along the loaded face, which was not found by Yettram and Robbins [5]. It can also be observed that as the eccentricity increases, the size of the spalling zone also increases.

In Figure 7(a), the variation of σ_y along the loaded face for different values of e at $k = 0.1$ and $\nu = 0.15$ is shown. It can be observed that as the value of e increases the magnitude of maximum transverse tensile stress also increases. On the other hand, the magnitude of maximum transverse compressive stress reduces with the increase in value of e . One very important observation can be made that the magnitude of σ_t (max) along loaded face is very much higher than the magnitude of σ_t (max) along the axis of loading for eccentric prestressing forces (see Figure 7 (b)). For example, at $e = 0.8$ the magnitude of σ_t (max) along loaded face is 2.57 (See Figure 7(a)) which is almost three times of the magnitude of σ_t (max) along the axis of loading (σ_t (max) = 0.88, See Figure 3). It can also be observed that, the difference between σ_t (max) along loaded face and along the loading axis increases with increase in e and very rapidly at higher values of e .

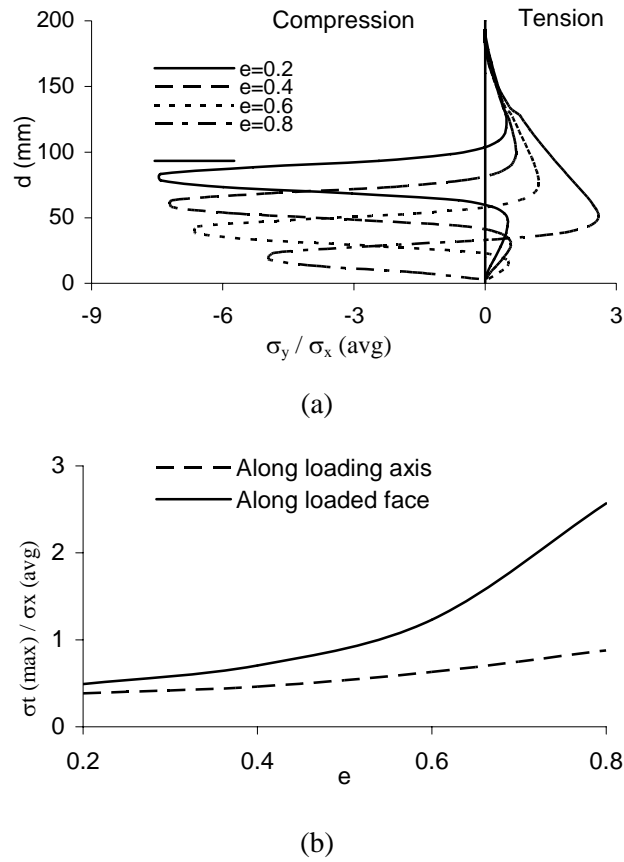


Figure 7. (a) Variation of σ_y along the loaded face (b) Comparison of variation in $\sigma_{t(max)}$ along the loaded face and along the axis of loading

7. Development of Parallel Solver

The prestressed post-tensioned concrete beam was discretized using 4800 three noded triangular elements with 2501 nodes each having two degree of freedom, hence resulting in global stiffness matrix of size 5002×5002 . To get the complete solution of the attempted problem, single processor of PARAM 10000 required 11.05 Hrs. The solution duration is very large because each processors of supercomputer PARAM 10000 operates at 400 MHz speed [11]. It was found that Total time required for complete solution of attempted problem was approximately 38 minutes. Therefore, a parallel solver was developed using parallel computing technique and Message Passing Interface (MPI) on the platform of supercomputer PARAM 10000 to save the computational time. Matrix Inversion Method was employed for the development of parallel solver for finding the inverse of sparse global stiffness matrix $[A]$. This inverse matrix $[A]^{-1}$ was then multiplied by known force vector $\{B\}$ to get the unknown displacement vector $\{X\}$. In the development of parallel solver, row wise data distribution among the processors was carried out, while column wise operations were carried out. Data

were distributed evenly among the processors to minimize computations. On the other hand, wherever the even data distribution was not possible, some processors with lower ranks were over loaded with excessive data. Figure 8 shows the parallel algorithm for parallel matrix inversion solver for finding solution of system of linear equations. The solver was then tested on different data sizes using different number of processors. It was found that this solver gave excellent performance on PARAM 10000 machine [14-15].

```

Global   $P$  {Number of Processors}
         $n$  {Number of Equations}
         $MyRank$  {Rank of the Processor}
         $Rank$  {Rank of processor holding current row}
         $start$  {Flag indicating starting row number for each processor}
         $end$  {Flag indicating ending row number for each processor }
         $i$  {Variable indicating current row}
         $[I]$  {Matrix indicating inverse of matrix  $[A]$ }
for all  $P_i$  where  $0 < i < P$  do
    Set  $start$ 
    Set  $end$ 
for  $i = 0$  to  $n-1$ 
    Set diagonal element of  $[A]_i = 1.0$ 
    Change elements of matrix  $[I]_i$ 
        for all  $P_i$  where  $0 < i < P$  do
            Find the  $Rank$  of current row
            If  $MyRank = Rank$ 
                Broadcast current row
            endif
        endfor
        for  $j = start$  to  $end$ 
            if  $[A]_{ij} \neq 0.0$ 
                Change non-diagonal element of  $[A]_{ij} = 0.0$ 
                Change elements of matrix  $[I]_{ij}$ 
            endif
        endfor
    endfor
    for  $i = start$  to  $end$ 
        Compute  $\{X\}_i$ 
    endfor
    for all  $P_i$  where  $0 < i < P$  do
        Broadcast  $\{X\}_i$  to All Processor
    endfor

```

Figure 8. Parallel algorithm for matrix inversion method

As communication among the processors plays a very important role in parallel computing technique, a small study was also carried out to study the different communication mechanisms. The above-mentioned parallel solver (Matrix Inversion Method) is developed using two communication mechanisms namely Blocking and Non-Blocking. A small study

was carried out on a data of size 1226×1226 and the Communication time was measured for different number of processors. Table 1 shows the variation in Communication time achieved by both communication mechanisms. It is very clear that the Communication time for both the communication mechanisms is nearly same and do not show significant difference in Communication time for any number of processors [15].

Table 1. Variation in Communication time with number of processors

No. of Processors	Communication time (Seconds)	
	Blocking	Non-Blocking
1	0.000000	0.000000
2	2.041498	3.378673
3	30.144950	24.633100
4	8.330960	6.825570
5	15.245690	16.615110

Table 2. Performance of FEA code on PARAM 10000

No. Of Processors	Computational time		Speedup	
	Total (Hours)	Communication (Minutes)	Actual	Ideal
1	11.046484	0.0000	1	1
2	5.5350045	1.0528	1.99575	2
3	3.6807758	3.0751	3.001129	3
4	2.8163307	2.6418	3.922297	4
5	2.4042693	3.9173	4.594529	5

8. Implementation of Parallel Solver in Fea

The above discussed Matrix Inversion parallel solver is incorporated in a FEA code, which is

capable of analyzing the 2-dimensional problems. The problem of prestressed post-tensioned concrete beam (see Figure 1) was analyzed using this code by increasing the number of processors of PARAM 10000 from one to five. Several analyses were carried out taking different values of k , e and ν and in every execution 480 MB of memory was utilized (see idealization of the problem). Table 2 shows the variation in the different components of computational time with increase in number of processors. It can be observed that Total time reduces considerably with the increase in the number of processors. For an instance, Total time of 11.04 Hrs. was reduced to 2.4 Hrs. by employing five numbers of processors. On the other hand, Communication time increases with the increase in number of processors by a small magnitude (0 to 4 minutes approximately), which is quite natural. Table 2 also shows the variation in Speedup achieved by the FEA code. It indicates that actual Speedup is very close to Ideal Speedup. Maximum Speedup achieved was 4.59 for five numbers of processors.

9. Conclusions

The paper presents a study of development of anchorage zone through stress development in prestressed post tensioned concrete beam using finite element analysis. Detailed parametric study has been reported by changing the parameters like loaded area ratio (k), Poisson's ratio (ν) and eccentricity (e) of prestressing force. The effect of these parameters on development of stresses and bursting force have been studied and discussed. A supercomputer PARAM 10000 was employed to carry out the simulations and to obtain the computational time variation with increasing number of processors. Several aspects from this study are worth noting.

1. Stress variation in anchorage zone was obtained and compared with available literature and found that results of present investigation have good agreement with previous studies (see Figure 2 (a)).
2. Study shows that Poisson's ratio affects the magnitude of bursting tensile force in prestressed post-tensioned concrete beam (see Figure 4 (a)).
3. Study shows that as the eccentricity of prestressing force increases, the magnitude of bursting tensile force reduces (see Figure 4 (b)).
4. An expression for computing the magnitude of bursting tensile force was developed incorporating the effect of Poisson's ratio. The results of developed equation was compared with the available literature and discussed. It was found that the equation given in Indian Standard Code IS: 1343-1980 computes maximum magnitude of F_{bst} .
5. Effect of eccentricity over the transverse tensile stress development in spalling zone was studied and it was found that stresses of very high magnitude were developed for the higher magnitude of the eccentricity. Hence it is advised that spalling zone should be carefully analyzed for prestressed post-tensioned beams subjected to eccentric prestressing forces.
6. Significant saving in computational time was achieved by employing parallel computing technique in Finite Element Analysis (see Table 2). It was also found that the obtained Speedup is very much near to the ideal Speedup.

Acknowledgements: The authors would like to thank the support of Image and Parallel Processing Lab., BITS, Pilani, INDIA, for providing parallel computing facilities for this work.

References

1. Zielinski J, Rowe RE. An investigation of the stress distribution in the anchorage zones of post-tensioned concrete members. *Cement and Concrete Association*, **13**(1962)573-82.
2. IS:1343-1980 Indian Standard Code of Practice for Prestressed Concrete. 1st Rev., Bureau of Indian Standards, New Delhi, 1981.
3. Iyengar KTS, Prabhakara MK. Anchor zone stresses in prestressed concrete beams. *ASCE Journal of Structural Division*, No. 3, **97** (1971) 807.
4. Iyengar KTS. Two dimensional theories of anchorage zone stresses in post-tensioned prestressed beams. *Journal of American Concrete Institute*, No. 10, **59**(1962)1443-66.
5. Yettram AL, Robbins K. Anchorage zone stressed in axially post-tensioned members of uniform rectangular section. *Magazine of Concrete Research*, No. 67, **21**(1969)103-12.
6. Byung-Wan Jo, Yunn-Ju Byun, Ghi-Ho Tae. Structural behavior of cable anchorage zone in prestressed concrete cable-stayed bridge. *Canadian Journal of Civil Engineering*, No. 1, **29**(2002)171-80.
7. Mackerle J. Finite and boundary elements and supercomputing - A bibliography (1989-1991). *Finite Elements in Analysis and Design*, No. 2, **12**(1992)151-9.
8. Shah MS, Kant T. Finite element analysis of fiber-reinforced polymer shells using higher order shear deformation theories on parallel distributed memory machines. *International Journal of Computer Applications in Technology*, No. 2, **12**(1999)206-10.
9. Khan AI, Topping BHV. Parallel finite element analysis using jacobi-conditioned conjugate gradient algorithm. *Advances in Engineering Software*, **25**(1996)309-19.
10. Thiagarajan G, Aravamuthan V. Parallelization strategies for element-by-element preconditioned conjugate gradient solver using high-performance fortran for unstructured finite-element applications on linux clusters. *ASCE Journal of Computing In Civil Engineering*, No. 1, **16**(2002)1-10.
11. <http://param.bits-pilani.ac.in>
12. Gupta PK , Khapre RN. Study of anchorage zone in post-tensioned concrete beams using finite element method. *Proceedings of the National Conference Advances in Civil Engineering Perspectives of Developing Countries*, HBIT, Kanpur, India, February 15-16,2003, pp.122-31.
13. Gupta PK, Khapre RN. Analysis of spalling zone in prestressed post-tensioned concrete beam using supercomputer PARAM 10000. *Proceedings of the National Conference Structural Engineering and Mechanics*, BITS, Pilani, India, September 24-25, 2004, p. 167.
14. Gupta PK, Khapre RN. Finite element analysis of anchorage zone using supercomputer PARAM 10000. *Proceedings of the International Conference Structural Engineering Convention, An International Meeting*, IIT, Kharagpur, India, December 12-14, 2003, p. 465.

15. Gupta PK, Khapre RN. Comparative Study of solution methods of system of linear equations on supercomputers. *Proceedings of the International Conference Structural Engineering Convention, An International Meet*, IIT, Kharagpur, India, December 12-14, 2003, pp. 522-30.

Symbols

σ_y	Transverse stress
σ_t	Transverse tensile stress
$\sigma_{t(max)}$	Maximum transverse tensile stress
$\sigma_{x(avg)} = P_k/d$	Average longitudinal stress
F_{bst}	Bursting tensile force
P_k	Applied prestressing force
k	Ratio of loaded area and cross-sectional area of the beam
e	Eccentricity of prestressing force
ν	Poisson's ratio
$a = 2d$	Length of beam
d	Depth of beam